

**E.B.S. Pardue Matlock**  
Technology for Energy Corporation (TEC)  
Knoxville, TN 37932

**M.R. James**  
Rockwell International  
Thousand Oaks, CA

**R.W. Hendricks**  
Virginia Polytechnic Institute and State University  
Blacksburg, VA

# Focusing Circle Errors in X-Ray Residual Stress Measurements of Nickel-Based Materials

## Introduction

An unexplained anomalous  $\sin^2\psi$  split in x-ray stress measurements has consistently resulted from the use of Cr  $K_\alpha$  radiation with nickel and austenitic stainless steels. Both materials have diffraction peaks at low back-reflection angles for this radiation (nickel:  $2\theta \sim 134^\circ$ , austenitic stainless steel:  $2\theta \sim 128^\circ$ ). The anomalous split is not evident when the measurements are made using Cr  $K_\beta$  radiation. In an attempt to explain the errors produced by the Cr  $K_\alpha$  radiation, focusing circle effects were analyzed and compared to experimental measurements made with both Cr  $K_\alpha$ , and Cr  $K_\beta$  radiation on nickel-based samples.

## Background

Some work has been done toward explaining and quantifying errors resulting from focusing circle effects when conducting x-ray stress measurements on a Bragg Brentano focusing diffractometer. Zantopulos and Jatzcak<sup>1</sup>, James and Cohen<sup>2</sup>, and more recently Hendricks<sup>3</sup>, working under an SBIR Program for Naval Air Systems Command<sup>4</sup>, have developed models for defocusing errors. The model developed by Hendricks considered the problem of deviation

of the sample from the focusing circle and was based on the following assumptions. The x-ray source is a point source; the detector has perfect resolution; all vertical divergences of the beam can be ignored; the sample surface is at the center of the diffractometer circle; and the incident x-ray beam has an angular divergence of  $2\alpha$ . Zantopulos and Jatzcak and James and Cohen made fewer assumptions with the concomitant result of more complicated analysis. The simpler Hendricks model will be used here, although analysis using the other models gives similar results.

As the sample (or diffractometer) is tilted through the  $\psi$  angles, the focusing circle changes and, thus, the detector position relative to the central ray does not move as the  $\psi$  angle varies, but all other rays are displaced to smaller  $2\theta$  values. The diffraction peaks at negative  $\psi$  angles are skewed more than for positive  $\psi$  angles and the peak positions are artificially shifted to smaller  $2\theta$  values. For a flat sample, this shift in the peak position between  $\psi = 0$  and  $\psi = \psi$  can be approximated by the following equation.<sup>3</sup>

$$\Delta 2\theta = \frac{-1r_{gc}(2\alpha)^2 \sin 2\theta}{3r_d 2! \sin^2(\theta + \psi)} \quad (1)$$

Where:

- $r_{gc}$  = radius of the goniometer circle
- $r_d$  = distance of detector from sample ( $r_d$  may or may not =  $r_{gc}$ ), and
- $2\alpha$  = angular divergence of the x-ray beam incident on the sample, in radians

In this simplified treatment, no attempt was made to correct for effects such as variations of the diffracted intensity with the Bragg angle or variations in the intensity of the incident beam. Analytical solutions to the equations for the focusing circle error show two trends. First, low angle back reflection diffraction peaks have a large peak position error when compared to high angle back reflection diffraction peaks. Second, the peak-position errors associated with negative  $\psi$  angles are substantially greater than those associated with positive  $\psi$  angles. This is important because of the increasing use of negative  $\psi$  tilts to check for  $\psi$  splitting due to shear stress or  $\psi$  misalignment.<sup>5</sup> These trends are illustrated in Figures 1 and 2 for both Cr  $K_\alpha$  ( $2\theta \sim 134^\circ$ ) and Cr



## Focusing Circle Errors in X-Ray Residual Stress Measurements of Nickel-Based Materials

$K_{\beta}$  ( $2\theta \simeq 158^{\circ}$ ) diffraction from nickel. These results clearly predict errors which may be large compared to the peak shifts expected in many x-ray residual stress measurements.

### Experimental Technique

To check the predictions of this theory, several measurements were made on a flat, nickel-plated sample and a flat, Monel 400 sample. The nickel-plated sample had a small tensile stress and the ground and polished Monel 400 sample had a large tensile stress. The samples were positioned and kept stationary while stress measurements were made using a TEC portable x-ray diffraction system and  $+\psi$  and  $-\psi$  tilts with  $\psi$ -angle oscillation.<sup>6</sup> On this instrument, focusing is not maintained since the detector is not moved radially. A series of measurements was made using Cr  $K_{\beta}$  radiation followed by Cr  $K_{\alpha}$  radiation with the samples remaining in the original position. Measurements were made for a range of positive and negative  $\psi$  angles. The Cr  $K_{\alpha}$  data were copied on computer diskettes, and the copied data were altered to include only the positive  $\psi$  angles. These data were then analyzed to give a comparison of the correlation coefficient of the d-spacing versus  $\sin^2\psi$  plots (expressed as an error in  $\sigma_y$ ) for the analyses containing both positive and negative  $\Psi$  angles versus those containing only positive  $\Psi$  angles. All data are shown in Table 1, and the nickel-plated sample data are illustrated in Figure 3.

The Cr  $K_{\beta}$  data were obtained at approximately  $158^{\circ} 2\theta$  for the {311} planes. The {220} planes resulted in diffraction peaks at approximately  $134^{\circ} 2\theta$  for the nickel plating and at approximately  $131^{\circ} 2\theta$  for the Monel 400 with Cr  $K_{\alpha}$  radiation. The x-ray elastic constants,  $(1+\nu)/E$ , used in these analyses were appropriately selected to reflect the set of planes being analyzed. Representative d-spacing versus  $\sin^2\Psi$  plots for the three Monel 400 cases are shown in Figures 4 through 6.

### Results and Discussion

The plot for Cr  $K_{\beta}$  radiation shows the negative and positive  $\Psi$  angles randomly located about the straight-line fit. In contrast, the plot for Cr  $K_{\alpha}$  radiation shows that all negative  $\Psi$  angle data have larger d-spacings (smaller  $2\theta$ ) than the positive  $\Psi$ -angle data. This results in the error calculated from the regression analysis being largest for the Cr  $K_{\alpha}$   $\pm\Psi$  case, that is, the case where the  $\Psi$  split is greatest. This split in the negative and positive  $\Psi$  angles conforms to effects predicted by the focusing circle analysis. To quantify these trends, the following example from the Monel 400 is given. At  $\sin^2\Psi = 0.3$ , the difference between  $\Psi = 33^{\circ}$  and  $\Psi = -33^{\circ}$  is  $\sim -0.07^{\circ} 2\theta$  from the theoretical calculation. The average  $\Delta 2\theta$  calculated from the Monel 400 data at  $\sin^2\Psi = 0.3$  is  $-11^{\circ} 2\theta$ . The error becomes even larger for higher  $\Psi$  tilts. These observations are consistent with the predictions of the theory.

The stresses calculated from the data indicate that the nickel-plated sample has a low tensile stress and the Monel 400 sample has a relatively high tensile stress. It is evident from Table 1 and Figure 3 that, although similar stresses were determined in each of the different tests, the error bars are improved considerably by using only the positive  $\Psi$  angles for Cr  $K_{\alpha}$  radiation or by using Cr  $K_{\beta}$  radiation. The error bars in these cases were attributed to nonlinearity caused by preferred orientation of the grains. The increased error bars associated with the measurements made with Cr  $K_{\alpha}$  radiation at both positive and negative  $\Psi$  angles were attributed to nonlinear d-spacing versus  $\sin^2\Psi$  plots, i.e.,  $\sin^2\Psi$  splitting.

The extreme negative and positive  $\Psi$  angles for both Cr  $K_{\alpha}$  and Cr  $K_{\beta}$  radiations were examined visually to determine whether skewed peaks were evident. Figures 7 and 8 show the negative and positive  $\Psi$  angles superimposed for both radiations. As expected the signal-to-noise ratio is lower for Cr  $K_{\beta}$  than for Cr  $K_{\alpha}$  radiation. Despite the noisy peaks for Cr  $K_{\beta}$  radiation, it is apparent that the negative and positive



## **Focusing Circle Errors in X-Ray Residual Stress Measurements of Nickel-Based Materials**

$\Psi$  angles have the same contours. On the other hand, the negative  $\Psi$  angle with Cr  $K_{\alpha}$  radiation is skewed relative to the positive  $\Psi$  angle.

The artificial shift in the negative  $\Psi$  angle is to a lower  $2\theta$  angle as predicted by the focusing circle analysis. Again, these observations are consistent with the predictions of the theory.

### **Conclusions**

Several worthwhile observations resulted from this work. When using  $\pm\Psi$  tilts, Cr  $K_{\beta}$  radiation produces superior stress data on the nickel sample when compared to the data obtained with Cr  $K_{\alpha}$  radiation. Cr  $K_{\alpha}$  radiation does produce satisfactory stress data when only the positive  $\Psi$  angles are used.

Low back-reflection diffraction peaks and negative  $\Psi$  angles result in errors in calculated stress. These errors can be predicted from focusing circle effects. For nickel, more precise stress data can be acquired using Cr  $K_{\beta}$  radiation at the high back reflection angle for  $\{311\}$  planes. Cr  $K_{\alpha}$  radiation gives similar stress results to Cr  $K_{\beta}$  radiation, but the errors are larger for Cr  $K_{\alpha}$  radiation. The errors in stress data with Cr  $K_{\alpha}$  radiation can be improved by using only positive  $\Psi$  angles.

### **Acknowledgments**

The authors gratefully acknowledge the technical assistance of Dr. B. S. Borie and are indebted to Ms. M. H. Mailhos for her editorial expertise in the preparation of this manuscript.

### **References**

1. H. Zantopulos and C. Jatzcak, "Systematic Errors in X-Ray Diffractometer Stress Measurements Due to Specimen Geometry and Beam Divergence," *Advances in X-Ray Analysis*, 14, 360-376 (1970).
2. M. R. James and J. B. Cohen, "Geometrical Problems with a Position Sensitive Detector Employed on a Diffractometer," *J. Appl. Crystallogr.* 12, 339-445 (1979).
3. R. W. Hendricks, to be published.
4. E. B. S. Pardue Matlock, Research and Development Program to Develop a Nondestructive Evaluation Instrument (X-Ray Diffraction) for Measuring Residual Stresses in a Wide Range of Naval Aviation Material, Final Report, TEC Report R87015, April 1987, Contract No. NOOO1985C0419.
5. I.C. Noyan and J. B. Cohen, "Determining Stresses in the Presence of Nonlinearities in the Interplanar Spacings Versus  $\sin^2\Psi$ ," *Adv. in x-ray Analysis*, 27, 129-148(1984).
6. M. R. James, "The Use of Oscillation on PSD-Based Instruments for X-Ray Measurement of Residual Stress," *Exp. Mech.*, 27, June 1987, No. 2, 164-167.
7. E. B. S. Pardue Matlock et al., "X-Ray Stress Analysis of Nickel-Plated Components," *Proceedings of the 1987 SEM Spring Conference on Experimental Mechanics*, 703-710.



## Focusing Circle Errors in X-Ray Residual Stress Measurements of Nickel-Based Materials

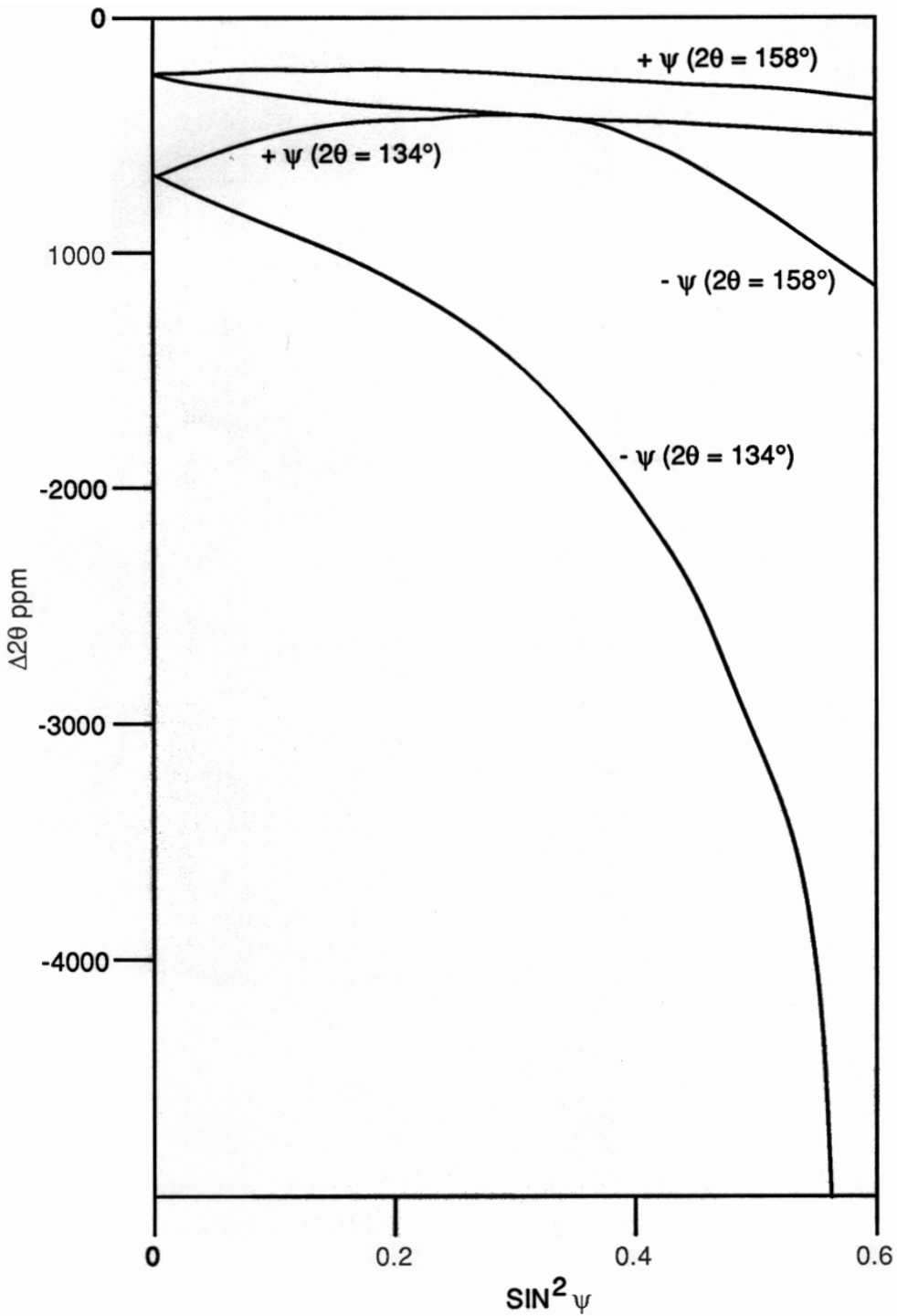


Figure 1 -  $\Delta 2\theta$  Versus  $\text{SIN}^2 \Psi$  for  $2\alpha = 4^\circ$ .

## Focusing Circle Errors in X-Ray Residual Stress Measurements of Nickel-Based Materials

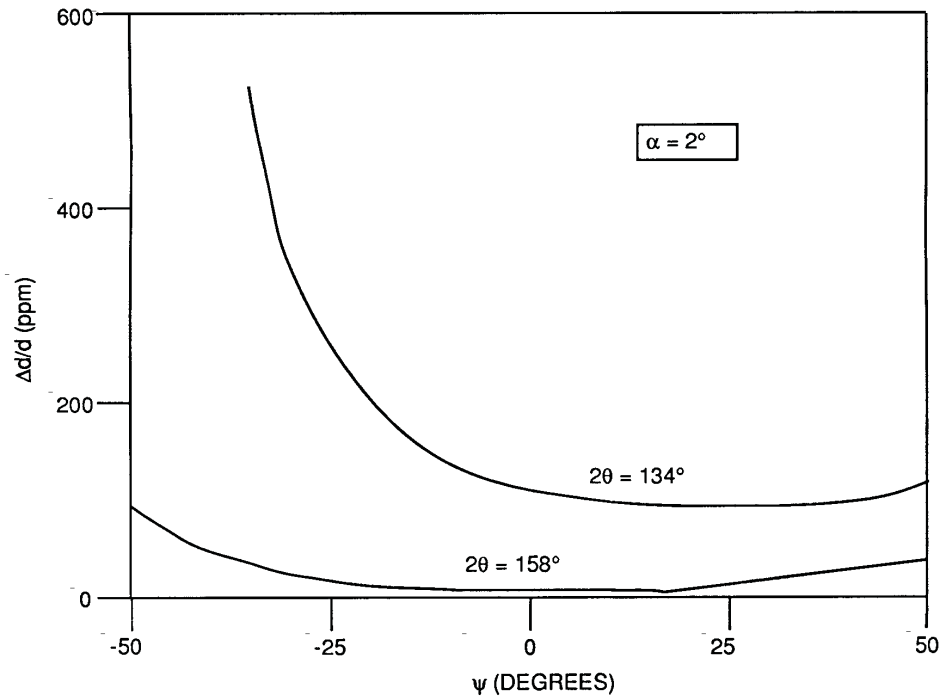


Figure 2. Plot of  $\frac{\Delta d}{d}$  for  $Cr K_{\alpha}$  ( $2\theta = 134^{\circ}$ ) and  $Cr K_{\beta}$  ( $2\theta = 158^{\circ}$ ).

TABLE 1 RESIDUAL STRESSES IN NICKEL AND MONEL 400 FOR $Cr K_{\alpha}$ AND $Cr K_{\beta}$ RADIATION		
MEASURED STRESS, MPA		
$Cr K_{\beta}$ ( $\pm\psi$ )	$Cr K_{\alpha}$ ( $\pm\psi$ )	$Cr K_{\alpha}$ (+ $\psi$ only)
<i>Nickel Plating</i>		
28.7 $\pm$ 29.3	37.8 $\pm$ 66.1	31.5 $\pm$ 29.3
12.6 $\pm$ 25.1	19.3 $\pm$ 63.8	10.4 $\pm$ 31.7
24.3 $\pm$ 19.4	24.4 $\pm$ 58.8	22.3 $\pm$ 40.2
21.9 $\pm$ 8.3	27.2 $\pm$ 9.6	21.4 $\pm$ 10.6
<i>Monel 400</i>		
360.5 $\pm$ 43.8	380.4 $\pm$ 70.1	408.7 $\pm$ 23.7
392.8 $\pm$ 44.5	376.2 $\pm$ 78.4	413.3 $\pm$ 39.0
376.8 $\pm$ 44.9	371.0 $\pm$ 70.2	400.6 $\pm$ 24.3
394.6 $\pm$ 21.4	361.6 $\pm$ 62.5	391.3 $\pm$ 35.1
410.6 $\pm$ 36.8	387.1 $\pm$ 57.7	407.8 $\pm$ 29.4
387.1 $\pm$ 19.1	375.3 $\pm$ 9.6	404.3 $\pm$ 8.6

Note: The error after each measurement is that from the correlation coefficient of the linear least-squares fit to the d-spacing versus  $\sin^2\psi$  data. Error in the average is the standard deviation over the replicate measurements.

## Focusing Circle Errors in X-Ray Residual Stress Measurements of Nickel-Based Materials

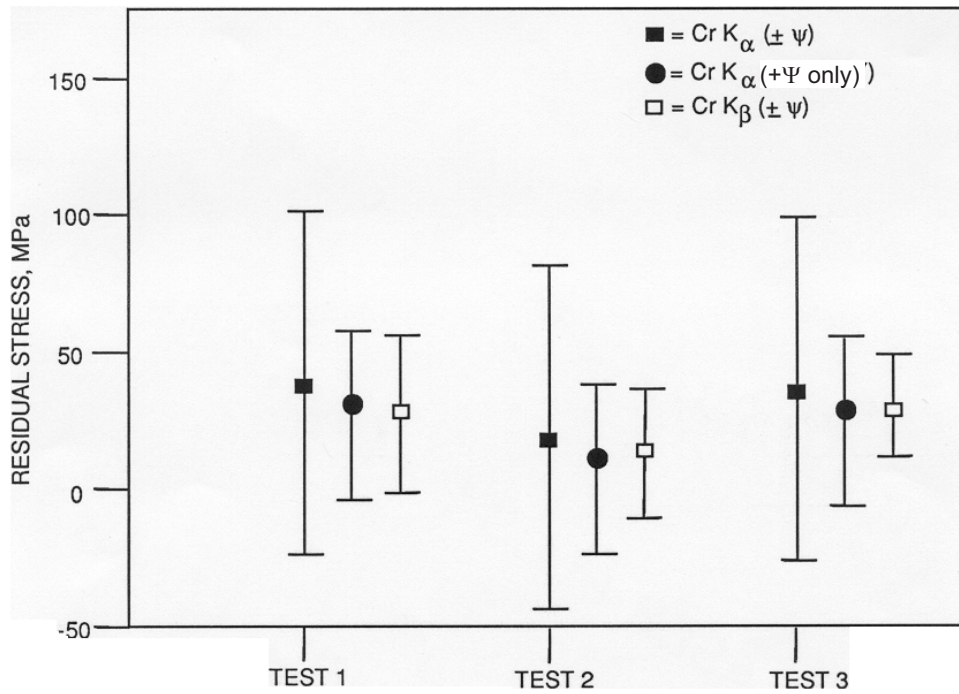


Figure 3 - Comparison of Cr K<sub>α</sub> and Cr K<sub>β</sub> Stress Data on Nickel Plating.

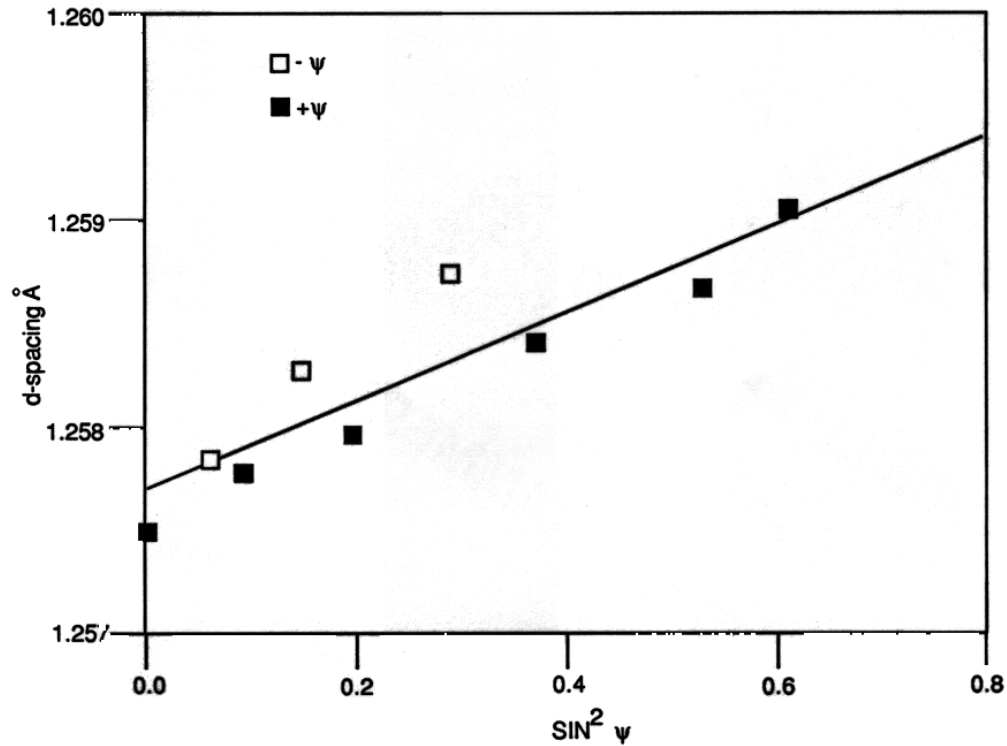


Figure 4 - d-Spacing Versus Sin<sup>2</sup>ψ Plot for Monel 400 Using Cr K<sub>α</sub> Radiation.

## Focusing Circle Errors in X-Ray Residual Stress Measurements of Nickel-Based Materials

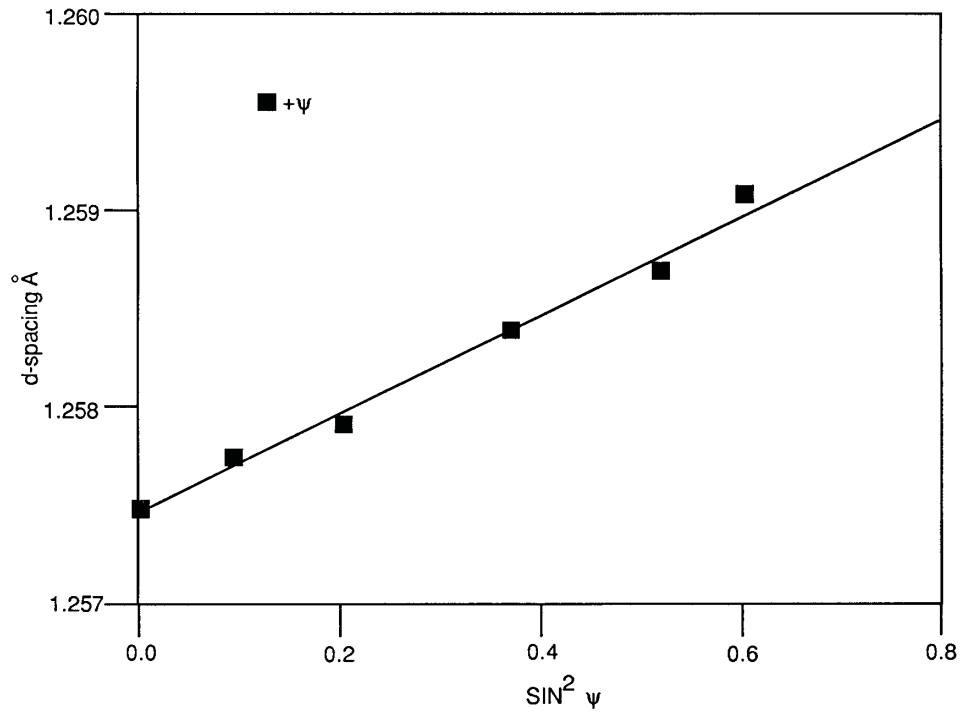


Figure 5 - d-spacing Versus  $\text{Sin}^2\Psi$  Plot for Monel 400 Using Cr  $K_\alpha$  Radiation (Positive  $\Psi$  Angles Only).

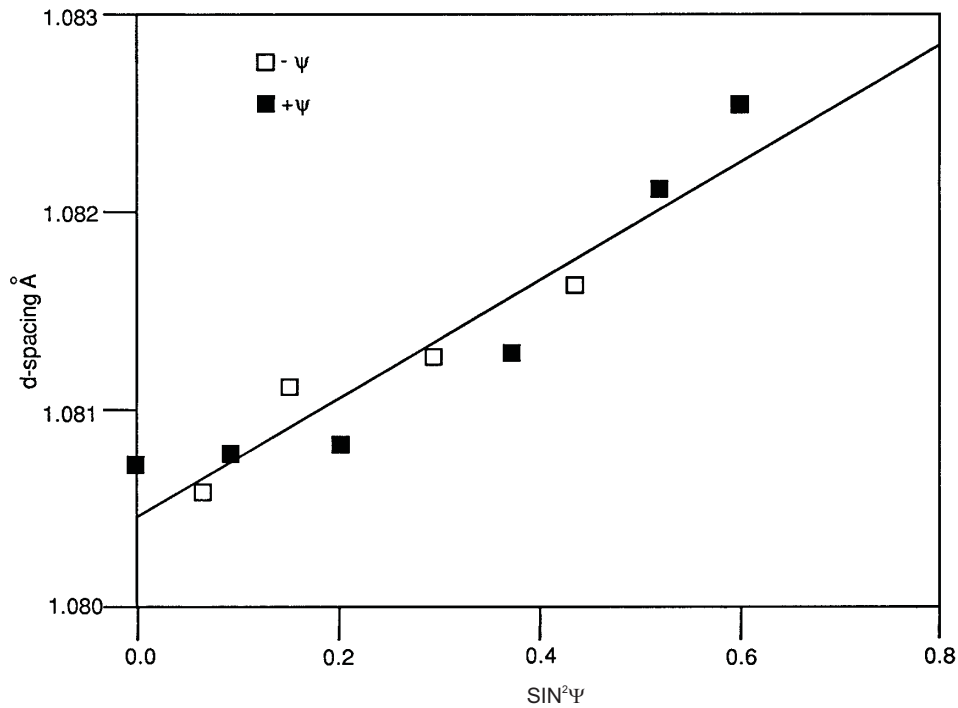


Figure 6 - d-spacing Versus  $\text{Sin}^2\Psi$  Plot for Monel 400 Using Cr  $K_\beta$  Radiation.

## Focusing Circle Errors in X-Ray Residual Stress Measurements of Nickel-Based Materials

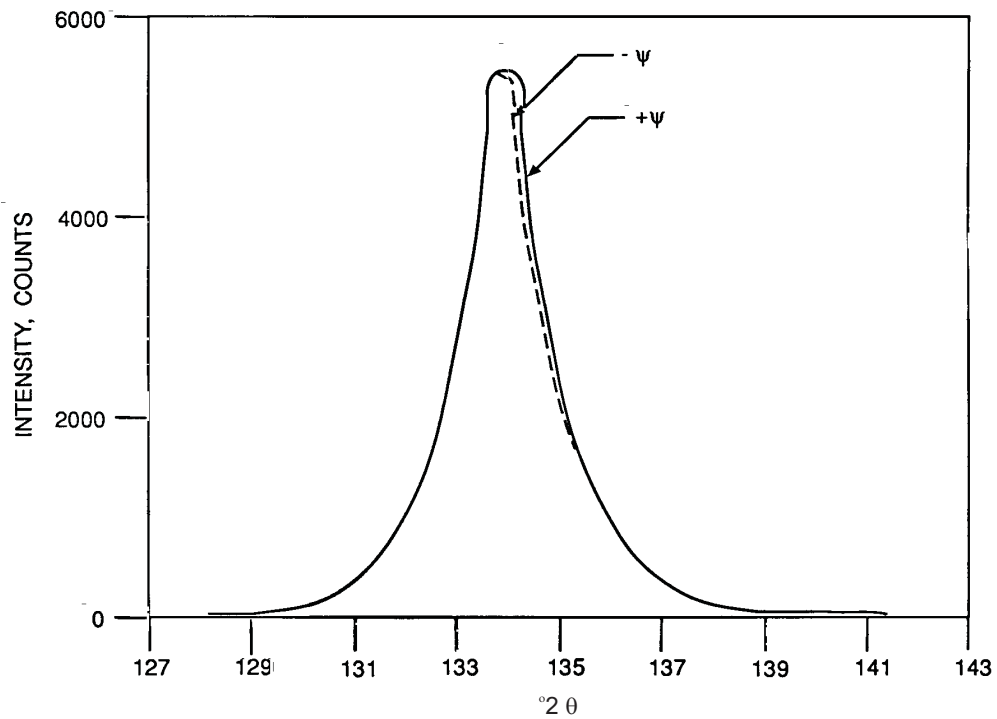


Figure 7 - Diffraction Peaks for Extreme Positive and Negative  $\Psi$  Angles Using  $\text{Cr K}_\alpha$  Radiation.

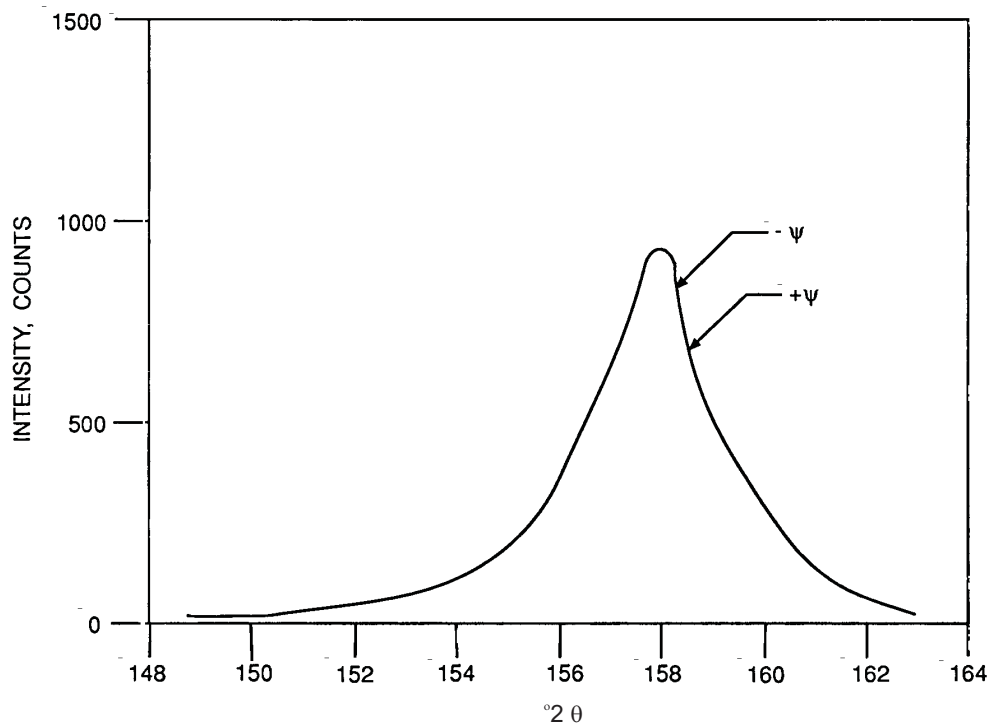


Figure 8 - Diffraction Peaks for Extreme Positive and Negative  $\Psi$  Angles Using  $\text{Cr K}_\beta$  Radiation.